# Ring-Coil Transitions in Nematic Ring Polymers: Monte Carlo Simulation

**Clive A. Croxton**

*Department of Mathematics, The University of Newcastle, New South Wales, Australia 2308*

*Received August 28, 1991; Revised Manuscript Received March 2, 1992*

ABSTRACT: A Monte Carlo simulation of small ($N \leq 20$) polynematic ring molecules is presented and comparisons are made with their linear counterparts. In particular, the order parameter $S$, number of hairpins, mean square radius of gyration, and ellipticity are investigated as a function of reduced temperature and stiffness. Ring-coil transitions and related phenomena are observed as the system passes through the nematic-isotropic transition temperature. Odd-even effects are investigated as the homologous sequence is ascended, and pronounced alterations in the magnitude of the parameters are observed with ring size and stiffness.

## Introduction

Numerous studies of semiflexible linear liquid crystal polymers have now been reported, reflecting the technological interest and application of these systems to materials science.[1-8] Two broad classifications may be identified, main chain and side chain, with an associated diversity and complexity of transitional behaviors depending upon the internal degrees of freedom available to the system. In the case of linear main-chain molecules, flexibility has generally been modeled as a linear sequence of stiff and less stiff sections in which flexibility is localized at junctions between adjacent rodlike sections or as a uniformly stiff (but not rigid) sequence in which flexibility is distributed homogeneously along its length. Such a system is termed a wormlike chain, characterized by a persistence length $\ell$. While both models embody essential features of realistic systems, they nevertheless represent caricatures amenable to theoretical analysis.

Treatments of the linear wormlike chains in the presence of an external potential have been presented by a number of authors on the basis of a variety of analyses with the general conclusion that the mean order parameter $S$ for the chain undergoes a first-order transition at some reduced temperature $T_{NI}$. For $T > T_{NI}$ a disordered or "coil" state arises, while for $T < T_{NI}$ a partially aligned or extended phase develops.

Associated configurational parameters such as the mean square end-to-end length $\langle R_{1N}^2 \rangle$ and the mean square radius of gyration $\langle S_N^2 \rangle$ reflect the transition in the order parameter, although the latter has a quadrupolar dependence upon backbone orientation with respect to the director field while $\langle R_{1N}^2 \rangle$ and $\langle S_N^2 \rangle$ are essentially dipolar in their dependence. As a result, the rod-coil and order-disorder transitions are not unequivocally related. The distinction between dipolar and quadrupolar dependence is particularly apparent for perfectly flexible jointed rod systems: we shall discuss this in more detail below.

Monte Carlo investigations of such systems have been less extensively reported,[9-12] despite their crucial role in assessing the status of the theoretical analyses based on the various caricatures of the realistic molecular systems. Of course, direct comparison with experiment may always be made; however, the idealizations necessary to carry through the theoretical analysis engenders some ambiguity in making a direct comparison.

In a recent series of papers,[4,7,13] Croxton has made immediate comparisons of the theoretical and Monte Carlo descriptions of the linear semiflexibly jointed rod model, *based upon parametrically identical models*. Apart from providing a direct assessment of the theory, the two approaches enable an unequivocal identification of the principal behavioral characteristics of the system. The theoretical description previously reported is based upon a correlation function approach, and the description is made in terms of the iterative convolution (IC) technique. The IC technique has been extensively described in the literature, and we refer the reader elsewhere for a detailed description.[13] Similarly, a Monte Carlo (MC) analysis of a parametrically identical system has been made, and the results have been compared. Here we extend those simulations to nematic *ring* polymers and, where appropriate, make detailed comparisons with their linear MC counterparts.

While a detailed review of our Monte Carlo linear jointed rod simulations is inappropriate here, a broad outline of the results is nevertheless of use, particularly since much of the motivation for the present investigation of polynematic rings derives from the results obtained from the linear simulations: the additional constraints and internal degrees of freedom available within the polynematic molecule provides a wealth of intriguing new phenomena when compared with our understanding of conventional low molecular weight mesogenic systems. In our MC simulations we investigated the development of the mean order parameter $S$, the mean square end-to-end length $\langle R_{1N}^2 \rangle$, the mean square radius of gyration $\langle S_N^2 \rangle$, and the mean number of hairpins $\langle n_H \rangle$ as a function of chain length and stiffness. It was noted that $\langle n_H \rangle$ had a central role in relating the dipolar quantities $\langle R_{1N}^2 \rangle$, $\langle S_N^2 \rangle$ to the quadrupolar order parameter $S$ for linear systems. Moreover, as previously suggested by de Gennes,[14] the development of hairpin states should exhibit an exponential dependence upon the reduced temperature of the system, and indeed we found that hairpins are progressively eliminated from the system, their number exponentially approaching zero with decreasing temperature. Given the central role of hairpins in our understanding of the orientational properties of linear polynematics, it is of interest to consider polynematic *rings*, for which of course, $n_H \geq 2$ even at the lowest temperatures. The effect that this constraint may have, together with the additional requirement that the chain must always form a closed loop, suggests that polynematic rings may exhibit somewhat more complex transitional phenomena, which we now proceed to investigate on the basis of Monte Carlo simulation.

0024-9297/92/2225-4352$03.00/0 

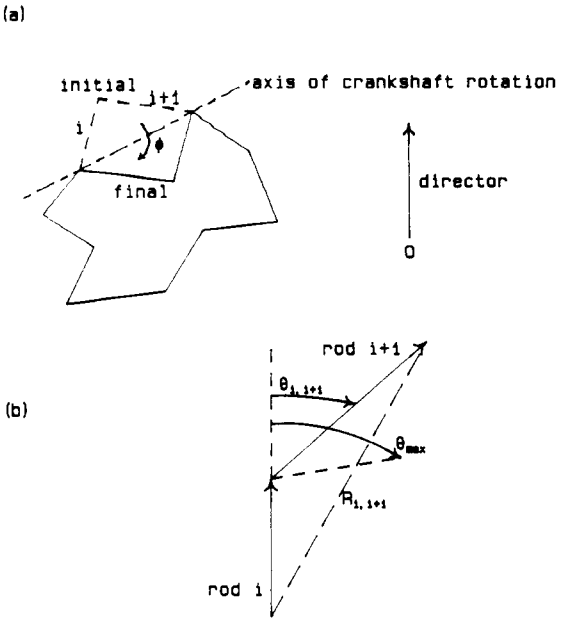


**Figure 1.** (a) Geometry of closed ring showing the random crankshaft rotation of two adjacent rods about their terminal links to the rest of the sequence. See Appendix 1 for a discussion of the variation of energy as the rotation $\Theta$ is made. (b) The cylindrically symmetric bend potential operating between adjacent links. We take $\Phi = 0$ (perfectly flexible) for $\Theta_{i,i+1} \leq \Theta_{max}$, $\Phi = \infty$ for $\Theta_{i,i+1} > \Theta_{max}$.

In presenting the current studies we emphasize that there are, to the best of our knowledge, no experimental examples of main-chain ring polymers with mesogenic units. However, this does not preclude their proposal and investigation: indeed, this forms the basis of the present simulation. Again, we are necessarily restricted to small rings for computational reasons when the closed loop constraint could well suppress the development of an oriented mesophase. The existence of such a mesophase will be identified as for their linear counterparts previously reported, that is in terms of the system's order parameter $S$. No attempt will be made here to anticipate long-chain behavior: we specifically restrict ourselves to short-chain mesogenic loops of varying flexibility.

## The Model and the MC Simulation Technique

We adopt a three-dimensional description of the chain and its interaction with the director field identical to that reported for our earlier MC analysis of linear systems,[13] with the additional requirement that the sequence forms a closed, connected loop without knots or entanglements (Figure 1a). We model the ring as a sequence of unit rods, flexibly connected such that the cylindrically symmetrical athermal bend potential between adjacent rods is given by (Figure 1b)

$$\begin{aligned} \Phi(\Theta_{i,i+1}) &= 0 \quad \Theta_{i,i+1} \leq \Theta_{max} \\ &= +\infty \quad \Theta_{i,i+1} > \Theta_{max} \end{aligned} \tag{1}$$

Clearly, $\Theta_{max}$ specifies the flexibility of the system, becoming a stiff rod when $\Theta_{max} = 0$ and totally flexible when $\Theta_{max} = \pi$. The unit rods provide a natural measure of the persistence length $\ell$, and to this extent our model coincides with Flory's description.[5] We number the rods sequentially from 1 to $N$, and designate the director by a vector 0. We may, therefore, specify the orientation of the $i$th rod with respect to the director by $\Theta_{oi}$, the entire system being assumed cylindrically symmetric about the vector 0. It should be realized that the angle between successive rods along the ring is restricted to $\Theta \leq \Theta_{max}$ in order to mimic the finite flexibility of the chain, and that over the allowed angular range of the junction, the bend potential is zero.

We work in the mean field approximation of Maier and Saupe who assumed

$$\Phi(\Theta_{oi}) = \frac{-AS}{2V^2}(3\cos^2\Theta_{oi} - 1) \tag{2}$$

for the orientational part of the potential energy of the $i$th rod with respect to the director. $V$ is the molar volume, $A$ is a constant taken to be independent of pressure, volume, and temperature,[15] and $S$ is the order parameter for the system defined as

$$S = \frac{1}{N}\sum_{i=1}^{N} S_i = \frac{1}{N}\sum_{i=1}^{N}\langle(3\cos^2\Theta_{oi} - 1)/2\rangle \tag{3}$$

where $S_i$ is the order parameter of the $i$th rod. The original Maier–Saupe representation (eq 2) of the orientational potential has been justified by a number of workers, although we should mention that Vroege and Odijk[8] have recently criticized this approach. The change in volume across the nematic–isotropic transition is so small that for present purposes we may regard it as constant and absorb it into the parameter $A$; moreover we prefer to work in terms of the reduced potential parameter $A^* = A/kT$, which we regard as a reciprocal temperature parameter, although $A^*$ bears the alternative interpretation as an isothermal density parameter.

As we have previously observed, simulation of semiflexible sequences of the type considered here presents an additional difficulty to those usually encountered in Monte Carlo simulation, and this arises from the fact that the chain–director interaction (eq 2) is a function of the (unknown) order parameter $S$. In our earlier linear polynematic simulations we approached the problem self-consistently, finding that value of $S$, at a given $A^*$, which when substituted in the potential function (eq 2) also yielded the same configurational average order parameter for the entire chain. We adopt the same procedure here for the polynematic rings; however, as Warner observed,[16] this is computationally expensive, and it might be more expedient to choose $A^*S = B$ in eq 2, determine $S$ by the usual method, and once settled deduce $A^*$. We refer the reader to our earlier paper[13] for details of the Monte Carlo procedure. However, the generation of new configurations in the case of a ring is somewhat different from that adopted for the simulation of linear sequences, as we shall now outline.

The requirement that new configurations of the sequence remain in a closed loop form enforces the adoption of "crankshaft" rotations of sections of the ring as shown in Figure 1a. This ensures that the loop remains sequentially connected while new configurations are rapidly generated. A subsequence of two adjacent rods within the $N$-mer is selected at random, and a random rotation $\pm\phi$ of the subset about the axis defined by its terminal junctions is made, subject of course to any flexibility restrictions (eq 1) (Appendix 1). Obviously such crankshaft rotations will result in variations of the configurational energy of the ring, and the usual Metropolis sampling technique may be applied. Since the remainder of the ring remains unmodified during any single rotation, successive configurations would be unacceptably strongly correlated. For a system of $N$ links, we choose a random $k$ ($1 \leq k \leq N^2$) and perform $k$ random rotations before counting the result as a new configuration. We use *batch* means rather than individual configuration values in estimating confidence intervals, since the theoretical basis

for these estimates presumes that the data measurements are normally distributed about a true mean value.[17,18] The various quantities we measure may or may not satisfy this condition if individual configurations are strongly correlated. There is, of course, an optimum batch size representing the balance between statistical adequacy and computational efficiency. We found that up to 500 configurations per batch were necessary to achieve a normal distribution of means.

Once the equilibrated value of $S$ has been determined it may be used in eq 4 and the statistics allowed to accrue in the course of estimation of the configurational properties of the system. Thus, the mean square length of a subsequence of rods $p$ ... $q$ within the ring is

$$\langle R_{pq}^2 \rangle = \left\langle \frac{\exp\left(-\sum_{i-1}^{N} \Phi_{oi}\right) R_{pq}^2}{\exp\left(-\sum_{i-1}^{N} \Phi_{oi}\right)} \right\rangle \quad (4)$$

and the mean square radius of gyration

$$\langle S_N^2 \rangle = \frac{1}{2N^2} \sum_p \sum_q \langle R_{pq}^2 \rangle \quad (5)$$

where $\langle\ \rangle$ denotes the configurational average determined on the basis of the batched statistics described above. We draw attention to our definition of the distance $R_{pq}$, which extends from one end of the $p$th rod to the other end of the $q$th.

## Results and Discussion

First, the order parameter $S$ for rings of $N = 10$ links was determined as a function of reciprocal temperature $A^*$ for various stiffnesses (Figure 2a). The comparable MC results for *linear* sequences of $N = 10$ rods are also shown (Figure 2b). The least flexible rings ($\theta_{max} \leq \pi/2$) are already severely constrained by the requirement that they form a closed loop and exhibit what can only be described as a sluggish response with increasing $A^*$ (decreasing temperature). Indeed, the nematic–isotropic transition is substantially compromised, and an orientationally ordered phase does not fully develop. Comparison with its linear counterpart (Figure 2b) in which an ordered phase develops for all systems, regardless of stiffness, suggests that the differing behavior is directly attributable to the closed ring requirement. With increasing flexibility ($\theta_{max} > \pi/2$) the system does appear to show a first-order phase transition between the isotropic and nematic phases and to this extent is similar to their linear counterparts. However, in the case of rings, both the onset of the transition ($A^*_{NI}$) and the asymptotic value of the order parameter at large $A^*$ is sensitively dependent upon ring flexibility.

For both linear and ring systems the location (or onset) of the transition shows a curious reversal in its location along the $A^*$ axis with increasing flexibility. This result was initially observed for the linear IC calculations and confirmed in the linear MC analysis. We believe this behavior is an idiosyncracy of the athermal bend potential adopted in these investigations (eq 1). The reversal with increasing flexibility may be regarded as an effective "stiffening" of the sequence in which adjacent rods may adopt the rigid, "bent open" configuration in complying with the nematic field.[13] Such configurations, even though they arise from highly flexible (large $\theta_{max}$) specifications, nevertheless behave stiffly in the bent open configuration. Less flexible sequences, while not able to assume the "open" but rigid configurations are still able to comply flexibly with the director field—indeed, more so than their a priori more flexible counterparts. This feature has been previously identified and discussed for linear systems.[13]

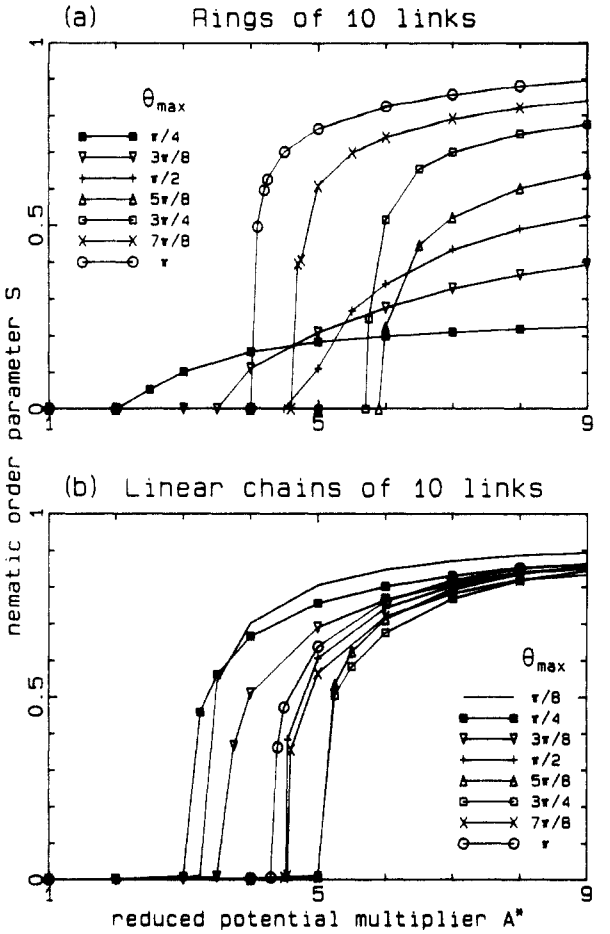


**Figure 2.** Monte Carlo order parameter $S$ for rings and linear chains ($N = 10$) as a function of reciprocal reduced temperature $A^*$ and stiffness $\theta_{max}$.

Qualitatively similar behavior is observed for larger rings. Again, the constraint that the sequence form a closed loop prevents the system from assuming a fully aligned phase, particularly for the stiffer rings and those for which $N$ is odd (see discussion of the odd–even effect below). However, as we might expect, compliance with the director is more complete at $N = 20$ for a given stiffness than its smaller counterpart with fewer degrees of freedom. The reversal in the location of the onset of the transition remains, however.

Having self-consistently settled the magnitude of the order parameter $S$ for a given ($A^*$, $\theta_{max}$) combination, the other configurational properties of the rings may be determined.

Comparison of the nematic order parameter $S(A^*)$ for rings and linear sequences (Figure 2) clearly shows the frustrated compliance with the director as stiffness increases. Indeed, for one of the stiffest rings investigated ($\theta_{max} = \pi/4$), we found $S_{ring} \approx 0.27$ at $A^* = 16$, while for its linear counterpart $S_{linear} \approx 0.88$ (both for $N = 10$). This behavior is readily understood, both in terms of stiffness and the reduced number of degrees of freedom associated with closing the sequence to form a ring. Of course, with increasing $N$ and the increasing number of degrees of freedom, the compliance with the director field will increase for any given stiffness and the asymptotic value of $S$ at large $A^*$ will accordingly increase. Both the rings

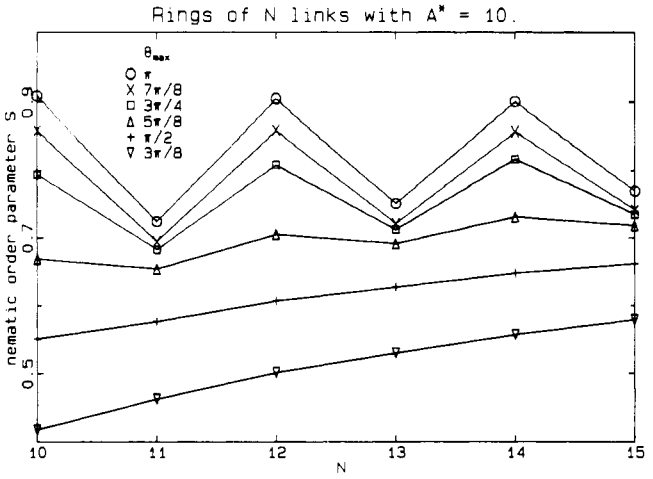


**Figure 3.** Odd-even effect on the order parameter for the homologous series $N = 10, 11, 12, \ldots$ at $A^* = 10$ for various stiffnesses. In all cases $A^* = 10$ corresponds to an ordered mesophase (Figure 2).

and the chains show the usual reversal in location of the transition $A^*_{NI}$ observed previously in the iterative convolution and Monte Carlo calculations for linear systems. The critical stiffness for reversal for this particular choice of bend potential appears to be ($\Theta_{max} \approx 3\pi/4$). However, as we mentioned previously, we make no proposals regarding the asymptotic behavior ($N \rightarrow \infty$) of the ring, nor do we attempt to identify any scaling laws and universal behavior.

**The Odd-Even Effect.** It has long been known for mesogenic systems of low molecular weight that a number of the characteristic features of the system such as the nematic–isotropic transition temperature, the order parameter, splay elastic constants, etc., show a pronounced alternation as the homologous series is ascended, that is, as the number of carbon atoms in the alkyl end chains is increased.[19] This is readily understood from a consideration of the molecular structure of the end chains for which the even members in, say, the trans conformation enhance the net molecular order while the odd members have the opposite effect. Such an effect would not arise for a perfectly flexible linear system, of course, nor for cylindrically symmetric linear sequences showing no preference for gauche or trans conformations, but it *does* arise for rings of all flexibilities and is attributed to the alternating degree of compliance of the rods in the ring with the nematic field, arising from the constraint that the sequence must form a closed loop. (In the case of rings it is this latter constraint which introduces an odd–even effect, which should be carefully distinguished from the odd–even phenomenon arising from rigid end-chain systems discussed above.)

The consequences of this effect for the order parameter at $A^* = 10$ for various stiffnesses is shown in Figure 3. For flexibilities $\Theta_{max} \geq 5\pi/8$ the rings show a pronounced odd–even effect with chain size in the nematic phase. This feature is readily understood in terms of the frustration of collapse and alignment of odd-numbered rings, while for stiffer systems ($\Theta_{max} \leq \pi/2$) the magnitude of the order parameter shows no odd–even effect, although there is a steadily increasing degree of compliance with the nematic field with increasing ring size and degrees of freedom. Over the short range of ring sizes investigated here it does appear from the data in Figure 3 that at a given stiffness the $S_{even}$ values show a linear increase with $N$, while the $S_{odd}$ values also show a different, but nevertheless linear $N$ dependence. Moreover, with increasing stiffness the $S_{even}$ and $S_{odd}$ loci gradually converge upon a single linear dependence on ring size. As we might expect, the linear loci of the $S_{even}$ and $S_{odd}$ values for a given ring stiffness gradually approach one another, suggesting that for sufficiently large rings having a large number of internal degrees of freedom the odd–even effect is no longer apparent. Other configurational properties of rings will also exhibit consequences of the odd–even effect, and we shall discuss them as they arise.

**Hairpins.** The role of hairpins in the description of linear polynematic systems had first been raised by de Gennes,[14] who presented a qualitative discussion of the thermal variation of the order parameter and length transitions in terms of $\langle n_H \rangle$, the mean number of hairpin reversals with respect to the director field axis. Clearly, the intrinsic stiffness of the chain implies a bending energy penalty for chain reversals executed in a small number of steps, while the external ordering potential disfavors transverse excursions across the nematic field. Evidently there is an energy, $E_H$, associated with the formation of a hairpin which in general has both bend and nematic components:

$$E_H = E_B + E_S \tag{6}$$

de Gennes expressed the probability of formation of a hairpin in Boltzmann form

$$\langle n_H \rangle \approx \exp(-E_H/kT) \tag{7}$$

and discussed its development in terms of thermal activation. Obviously, for those regions in which the order parameter $S = 0$ (i.e., $A^* < A^*_{NI}$), the nematic energy $E_S = 0$: only when $S > 0$ will contributions to the hairpin energy arise from this source. Generally, of course, the bend energy $E_B > 0$ for all $A^*$, although for our idiosyncratic choice of bend potential (eq 1), only those configurations for which $E_B = 0$ are allowed to develop. Accordingly, for the present simulations we have

$$E_H = 0 \qquad A^* < A^*_{NI}$$

$$E_H = E_S \qquad A^* \geq A^*_{NI} \tag{8}$$

which provides some simplification in the analysis.

We identify a hairpin as a configuration for which $\cos\Theta_{o,i} \cos\Theta_{o,i+1} < 0$—that is, a reversal of the chain backbone with respect to the external vector 0 (Figure 1). It should be noted that our identification of a hairpin does not necessarily imply a sharp reversal. Indeed, for stiff sequences chain reversals will in general be spatially extended structures. However, at *some* point in the reversal the condition $\cos\Theta_{o,i} \cos\Theta_{o,i+1} < 0$ will be satisfied and a hairpin indentified.

The crucial role of hairpins in reconciling the various ordering and configurational properties of linear systems has been discussed elsewhere.[4,7,13] In that analysis the order–disorder and rod–coil transitions were investigated and the superficially disparate behaviors reconciled in terms of the development of hairpin states which proved central to our understanding of linear polynematics. In the case of rings we necessarily have $n_H \geq 2$, whereas for linear chains we have $n_H \geq 0$. In Figure 4a we plot ln $(\langle n_H \rangle - 2)$ vs ln $A^*$ for $N = 10$ rings of various stiffnesses. In all cases $\langle n_H \rangle$ is independent of $A^*$ in the isotropic phase ($A^* < A^*_{NI}$) for our particular choice of bend potential, although the number $\langle n_H \rangle - 2$ is a sensitive function of ring stiffness. Again, the onset of thermal elimination of hairpins with $A^*$ corresponds closely to the location of the isotropic–nematic transition shown in Figure 2a. The roughly linear decrease in ln $A$ ($\langle n_H \rangle - 2$)

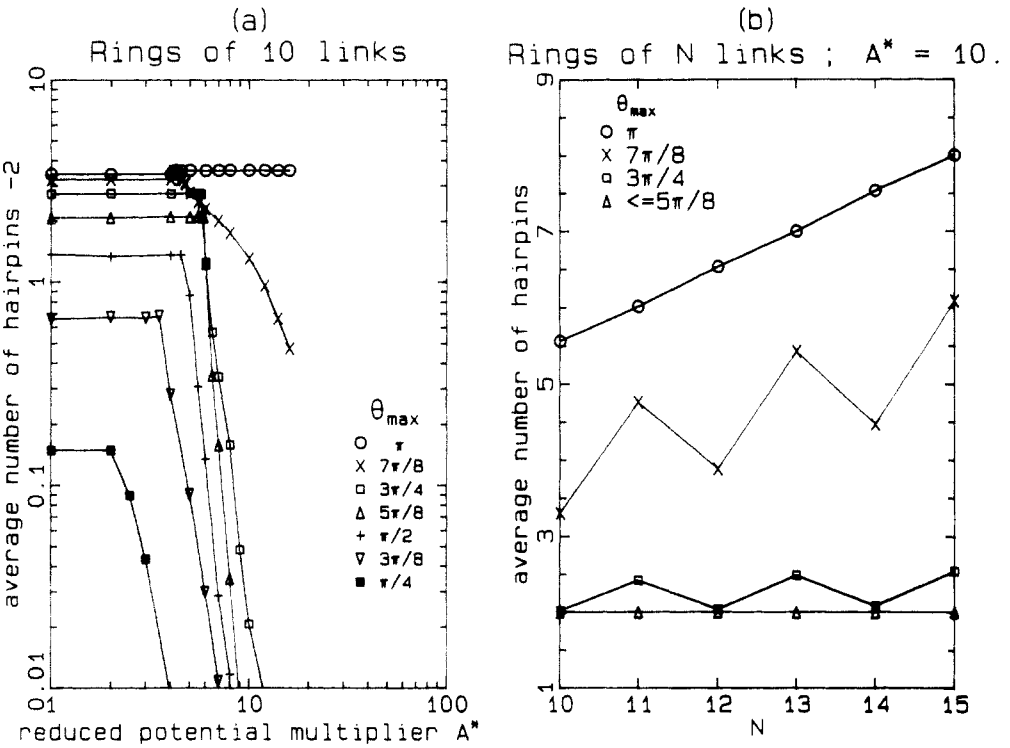


**Figure 4.** (a) log–log plot of average number of hairpins $\langle n_H \rangle - 2$ vs $A^*$ for $N = 10$ rings of various stiffnesses. (b) Odd–even effect on the average number of hairpins $\langle n_H \rangle$ for the homologous series $N = 10, ..., 15$ for various stiffnesses.

with ln $A^*$ once the transition is complete confirms the exponential relation of eq 7, while their generally parallel form suggests that the total nematic energy $E_H = E_S$ per ring is largely independent of stiffness. However, the energy per hairpin $\sim E_S/\langle n_H \rangle$ within the ring increases strongly with stiffness, and the onset of thermal elimination of the hairpins again shows the reversal with stiffness reported above for the order parameter.

Of particular interest are the fully flexible rings ($\theta_{max} = \pi$) which, like their linear counterparts, appear totally independent of $A^*$. Since no bend constraints apply in this case, the rods may fully comply with the external field (confirmed by the order parameter curve), in which case $E_H = E_S = 0$, and no thermal elimination may occur. The curious small discontinuous increase in $\langle n_H \rangle$ at $A^*_{NI}$ for perfectly flexible rings appears to be a real result. Simulations were repeated several times with the same outcome. We do not have an explanation for this feature. A comparison of the plots for rings of size $N = 10$ and 20, respectively, reveals parallel slopes for systems of identical stiffness. This implies identical activation energies for the thermal elimination of hairpins regardless of ring size, at least for the range of sizes investigated here. Of course, the *number* of hairpins for rings of a given stiffness depends sensitively upon $N$, but the *rate* at which they are eliminated depends only upon stiffness.

For relatively stiff rings ($\theta_{max} < 5\pi/8$) only minor buckling can occur and over the homologous range investigated here $\langle n_H \rangle$ remains $\sim 2$, reflecting the stiff ringlike structure (Figure 4b). With increasing flexibility, however, a pronounced odd–even effect develops. As might be expected for these more flexible systems, $\langle n_H \rangle$ gradually increases with $N$ showing an essentially linear dependence for perfectly flexible systems ($\theta_{max} = \pi$).

**Radius of Gyration.** The mean square radius of gyration of the rings is defined by eq 5 and shows a range of variation with $A^*$ which appears sensitively dependent upon stiffness (Figure 5a). For comparison, the linear counterparts are shown (Figure 5b), and apart from the qualitatively similar behavior in both cases, we note in particular that the stiffest and most flexible systems appear independent of $A^*$. In the case of the stiffest systems, the constraint of ring closure restricts compliance with the director to minor buckling with minimal consequences

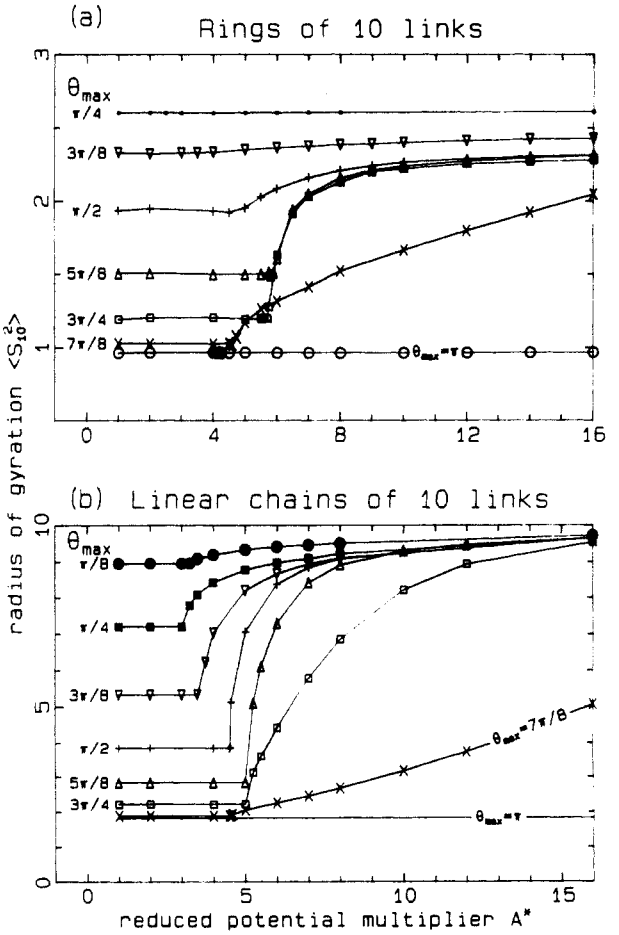


**Figure 5.** Dependence of the radius of gyration $\langle S_N^2 \rangle$ upon $A^*$ for $N = 10$ rings and linear chains ($N = 10$) of various stiffnesses.

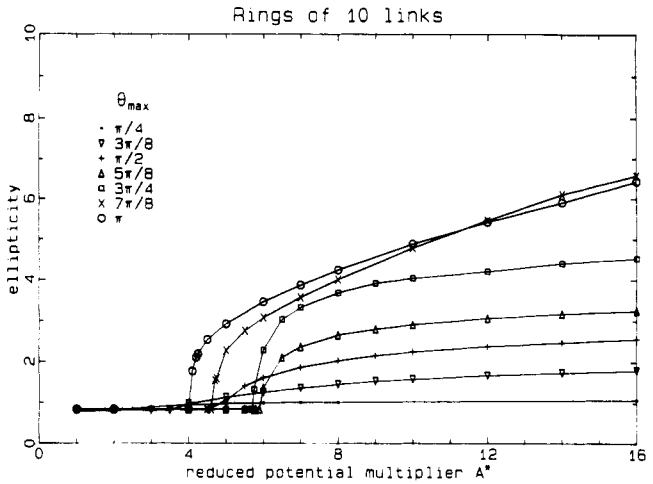


**Figure 6.** Ellipticity of a ring ($N$ = 10) (eq 9) as a function of $A^*$ for various stiffnesses.

for the radius of gyration even at the highest $A^*$ investigated here. For fully flexible rings, compliance with the nematic field does *not* necessarily imply any elongation of the ring, and while the order parameter $S$ and the ring ellipticity (see below) may develop strongly with $A^*$ (Figure 6), $\langle S_N^2 \rangle$ does not. At intermediate flexibilities there is a progressive interrelation between compliance with the external field and elongation of the ring, and this is reflected in the development of the ellipticity of the ring.

As we may readily appreciate, the additional internal degrees of freedom within the $N$ = 20 rings permit a more complete compliance with the director field at a given stiffness than does its smaller counterpart ($N$ = 10). Nevertheless, $\langle S_N^2 \rangle$ for the stiffest and fully flexible systems remain essentially independent of $A^*$ over the range investigated. It is appropriate to point out that the order parameter bears a quadrupolar relationship to the director field, while that of the radius of gyration is dipolar, accounting for the superficially disparate behaviors of the two quantities.

As we have already seen, thermal elimination of hairpins proceeds with increasing $A^*$ for all stiffnesses $\Theta_{max} < \pi$. The only case for which no thermal elimination can occur is for the perfectly flexible ring ($\Theta_{max} = \pi$). With thermal release of entrapped hairpins the system reorganizes itself to achieve the $n_H$ = 2 condition, corresponding to an open ring. This loop–coil transition would appear to correspond closely to the rod–coil transition previously reported for linear systems. In both cases there is an associated increase in the radius of gyration. This behavior is confirmed in Figure 5a, although the perfectly flexible system again warrants further comment. As we have already observed, there is no thermal elimination of hairpins for such systems and, accordingly, no development of $\langle S_N^2 \rangle$ with $A^*$.

A comparison of the radii of gyration $\langle S_{10}^2 \rangle$ as a function of $A^*$ for rings and chains (Figure 5a,b) shows them to be qualitatively similar. The results are essentially bracketed in both cases by the stiffest and most flexible curves, between which $\langle S_{10}^2 \rangle$ shows its usual reversal in the location of the transition $\Theta_{max} \approx 3\pi/4$. As expected, the *magnitudes* of $\langle S_{10}^2 \rangle$ for rings is somewhat smaller than their linear counterparts.

The odd–even effect on the radius of gyration of the rings as the homologous series is ascended reveals that the stiffest and most flexible systems show a linear increase with $N$: only for intermediate flexibilities is a clear odd–even effect apparent. As in the previous cases, the stiffest systems exhibit negligible compliance with the director field with increasing $N$, while the totally flexible rings comply fully with increasing $N$.

**Ring Ellipticity.** The mean ellipticity of the rings is defined as

$$\langle \epsilon \rangle = \langle L_z / \sqrt{L_x^2 + L_y^2} \rangle \tag{9}$$

where $L_z$, $(L_x^2 + L_y^2)^{1/2}$ denote the maximum spatial extent of the ring parallel and perpendicular to the director, respectively, about which the system is cylindrically symmetric. In the isotropic phase we would expect $\langle \epsilon \rangle$ to be $1/\sqrt{2}$, while progressive elongation of the ring with increasing $A^* > A^*_{NI}$ will be reflected in a corresponding increase in $\langle \epsilon \rangle$. Again, ring stiffness will frustrate compliance with the director field, as will the odd–even effect. The onset of elongation shows the usual reversal of its location along the $A^*$ axis with increasing flexibility (Figure 6).

Thermal elimination of hairpins toward the minimum hairpin condition $n_H$ = 2 with increasing $A^*$ implies a progressive transition (at least for $A^* > A^*_{NI}$ for the present choice of bend potential (eq 1)) from a coil to an elliptical ring whose major axis will coincide with the director field. For the stiffest rings ($\pi/4 \leq \Theta_{max} \leq \pi/2$) investigated, a loop state ($\langle n_H \rangle$ = 2) of low ellipticity is rapidly attained with increasing $A^*$. For these relatively stiff systems, the development of the ellipticity is achieved largely through minimal buckling and distortion of the ring. With increasing flexibility, however, the decrease in $L_x$ and $L_y$ arising from compliance with the director field results in a strong development of the ellipticity with $A^*$ depending upon stiffness (Figure 6). At large $A^*$ (Figure 6, $A^*$ = 16, for example) the ellipticity increases steadily in magnitude with increasing flexibility, yet with a seemingly anomalous *decrease* in magnitude for perfectly flexible systems. It would seem that there is some reversal in the magnitude of the ellipticity at large $A^*$ for highly flexible rings having $7\pi/8 < \Theta_{max} \leq \pi$. This we understand as the ability of highly flexible rings to repeatedly double back along the director, with an associated large number of hairpins, thereby reducing $L_z$ and lowering the ellipticity (Figure 6). Less flexible rings, with their dramatically smaller number of hairpins at large $A^*$ (Figure 4) can only comply with the director field by elongation and, hence, an increase in their mean ellipticity. We see that for the stiffest rings the odd–even effect on the ellipticity is minimal, although there is a gradual increase in the magnitude of $\langle \epsilon \rangle$ as $N$, and the number of degrees of freedom, increase. The odd–even effect develops markedly with increasing flexibility until for the most flexible systems ($\Theta_{max} = \pi$) the *magnitudes* show a reversal, while the saw-tooth effect continues to develop. This reversal in magnitude for highly flexible systems has been discussed above. Nevertheless, the development is alternately frustrated or assisted as $N$ is odd or even, and $\langle \epsilon \rangle$ accordingly shows a pronounced odd–even effect for more flexible systems.

**Acknowledgment.** I am indebted to Ruby Turner for the numerical computations and to the ARGS for financial support.

## Appendix 1

A sequence of random values $\{X\}$ can be generated having any desired probability distribution function:

$$F(x) = \text{probability that } X \leq x$$

The only restrictions on $F$ are that it must be nondecreasing and normalizable so $F(-\infty) = 0$, $F(+\infty) = 1$.

When dealing with a continuous probability

$$F(x) = \int_{-\infty}^{x} f(t)\, dt$$

where the density function $f(t)$ is nonnegative; again normalize so $F(+\infty) = 1$.

The desired $\{X\}$ is found by generating a uniform random sequence $\{Y\}$ and setting $X = F^{-1}(Y)$.

Because we are dealing with a function of angle we replace $-\infty$ with $\phi_0$ and $+\infty$ with $\phi_0 + 2\pi$. For convenience choose $\phi_0 = 0$ (it makes no difference to the result).

Our density function before normalization is

$$f(\phi) = e^{-(\phi_i + \phi_{i+1})}$$

where

$$\Phi_k = A^*S \frac{(1 - 3\cos^2 \theta_{0k})}{2}$$

and $\phi$ is as in Figure 1a. (Because the normalization factor is $\int_0^{2\pi} f(\Phi)\, d\phi$ we can use $\Phi_i + \Phi_{i+1}$ instead of $\Delta\Phi_i + \Delta\Phi_{i+1}$

$$e^{-(\Phi_i - \Phi_i' + \Phi_{i+1} - \Phi_{i+1}')} = e^{\Phi_i' + \Phi_{i+1}'} e^{-(\Phi_i + \Phi_{i+1})}$$

and the common constant factor can be taken out of both numerator and denominator.) Clearly $\theta_{oi}, \theta_{o,i+1}$ (and hence $\Phi_i$, $\Phi_{i+1}$) depend on both $\mathbf{R}$ and $\phi$ in fairly complex ways, so we resort to numerical integration.

Using a step-length of $2\pi/64$, $F^{-1}(Y)$ becomes $2\pi k/64$ for the smallest $k$ such that

$$\sum_{\ell=0}^{k} e^{-(\Phi_i(\mathbf{R},\ell) + \Phi_{i+1}(\mathbf{R},\ell))} \geq Y \sum_{\ell=0}^{63} e^{-(\Phi_i(\mathbf{R},\ell) + \Phi_{i+1}(\mathbf{R},\ell))}$$

To avoid utilizing enormous amounts of computer time calculating exponentials, we approximate $(\Phi_i + \Phi_{i+1})/A^*S$ to the nearest $^1/_{64}$ and use a lookup table.

Finally, having chosen $\phi$, we calculate $\theta_{i-1,i}$ and $\theta_{i+1,i+2}$. If these violate restrictions on the maximum bond angle the move is rejected and we try again, beginning with random choice of $i$.

## References and Notes


(1) Jähnig, F. *J. Chem. Phys.* **1979**, *70*, 3279.
(2) ten Bosch, A.; Maissa, P.; Sixon, P. *J. Phys. Lett.* **1983**, *44*, L105.
(3) Warner, M.; Gunn, J. M. F.; Bumgartner, A. B. *J. Phys. A: Math. Gen.* **1985**, *18*, 3007.
(4) Croxton, C. A. *Polym. Commun.* **1990**, *31*, 45.
(5) Flory, P. *Adv. Polym. Sci.* **1984**, *59*, 1.
(6) Wang, X.-J.; Warner, M. *J. Phys. A: Math. Gen.* **1986**, *19*, 2215.
(7) Croxton, C. A. *Macromolecules* **1990**, *23*, 2270.
(8) Vroege, G. J.; Odijk, T. *Macromolecules* **1988**, *21*, 2848.
(9) Bluestone, S.; Vold, M. J. *J. Chem. Phys.* **1965**, *42*, 4175.
(10) de Vos, E.; Bellemans, A. *Macromolecules* **1974**, *7*, 809.
(11) Baumgartner, A.; Yoon, D. Y. *J. Chem. Phys.* **1983**, *79*, 521.
(12) Khalatur, P. G.; Papulov, Yu. G.; Pletneva, S. G. *Mol. Cryst. Liq. Cryst.* **1985**, *130*, 195.
(13) Croxton, C. A. *Macromolecules* **1991**, *24*, 537.
(14) de Gennes, P.-G. In *Polymer Liquid Crystals*; Ciferri, A., Krigbaum, W. R., Meyer, R. B., Eds; Academic: New York, 1982; Chapter 5.
(15) Chandrasekhar, S. *Liquid Crystals*; Cambridge University Press: Cambridge, England, 1980; p 46.
(16) Warner, M., private communication, 1990.
(17) Bevington, P. R. *Data Reduction and Error Analysis for the Physical Sciences*; McGraw-Hill: New York, 1969.
(18) Bishop, M.; Frinks, S. *J. Chem. Phys.* **1987**, *87*, 3675.
(19) Marcelja, S. *J. Chem. Phys.* **1974**, *60*, 3599.